International Journal of Computer Science and Information Technology
ISSN: 3005-9682 (Print), ISSN: 3005-7140 (Online) | Volume 8, Number 5, Year 2026
DOI: https://doi.org/10.62051/ijcsit.v8n5.05
Journal homepage: https://wepub.org/index.php/IJCSIT/index

A Phenotype-Constrained Multi-objective Algorithm for Programmable Metamaterial Insole Design

Chenglin Xing [1], Peng Zeng [2], Xuezheng Yue [1, *]

[1] School of Materials and Chemistry, University of Shanghai for Science and Technology, Shanghai, China
[2] School of Mechanical and Energy Engineering, Beijing University of Technology, Beijing, China
*Corresponding Author: Xuezheng Yue

ABSTRACT

Personalized insoles are commonly designed from foot geometry or local pressure magnitudes, yet these approaches do not directly translate plantar loading phenotypes into region-specific mechanical functions. Programmable metamaterials based on triply periodic minimal surface (TPMS) architectures provide a tunable design space for stiffness, compliance, load capacity, and energy absorption, but a transparent mapping algorithm is needed to connect plantar pressure phenotypes with suitable regional structures. Here we introduce MetaInsole Mapper, a phenotype-constrained multi-objective algorithm for assigning TPMS structures to heel, midfoot, and forefoot regions. The framework encodes three quiet-standing plantar pressure phenotypes as regional demand vectors spanning cushioning, support, stability, and compliance. A TPMS mechanics database containing 24 candidate structures is transformed into normalized mechanical feature vectors, and candidate assignments are optimized using a demand-weighted score with printability and adjacent-region stiffness-transition penalties. MetaInsole Mapper generated phenotype-specific regional designs for heel-load exposure, high-variance postural-control, and balanced-control phenotypes. Compared with random assignment, uniform TPMS assignment, and a pressure-only rule, the proposed method achieved the lowest demand-matching error (0.5605) and the highest functional score (1.2440), while maintaining full regional specificity. Sensitivity analysis showed stable assignments under +/-5% and +/-10% demand perturbations and high overall stability under +/-20% perturbation (0.9333). These findings support MetaInsole Mapper as a reproducible computational bridge between plantar pressure phenotyping and programmable metamaterial insole design. The present study establishes an algorithmic design workflow; future work should validate the assigned structures through fabrication, bench testing, and human wear studies.

KEYWORDS

Plantar Pressure; Foot orthosis; Programmable Metamaterial; TPMS; Lattice Structure; Multi-objective optimization; Personalized insole; Computational Design

1. INTRODUCTION

Personalized insoles and foot orthoses are widely used to redistribute plantar loads, improve comfort, and support functional alignment during standing and gait [10, 12]. Traditional customization workflows often begin from foot shape, clinical impression, or localized pressure measurements. These inputs are useful, but they do not by themselves define how the mechanical behavior of an insole should vary across the heel, midfoot, and forefoot. A high heel cumulative-load phenotype, for example, implies a different regional mechanical objective from a phenotype dominated by postural-control variability. If these functional differences are not explicitly encoded, two individuals with

distinct plantar loading strategies may receive geometrically customized devices with similar mechanical behavior.

Plantar pressure analysis provides a functional description of foot-ground interaction [10]. Regional pressure, pressure-time integral, load distribution, temporal variance, and center-of-pressure descriptors can characterize how load is shared and stabilized across the foot. Footprint- and pressure-derived regional measures, including arch-related indices, have also been used to summarize structural and functional aspects of plantar loading [11]. Prior work on in-shoe pressure measurement, custom footwear, and orthotic materials has shown that pressure-guided design can reduce plantar pressure and inform offloading strategies, particularly in populations at risk of tissue overload [1, 2, 12]. However, many pressure-guided workflows remain rule-based: regions with higher pressure are assigned more cushioning or relief, while lower-pressure regions receive less intervention. Such rules are interpretable, but they may overlook multivariate phenotypes in which load magnitude, temporal variability, support demand, and compliance demand interact.

Additive manufacturing creates an opportunity to move beyond homogeneous orthotic materials. Lattice and TPMS structures can be fabricated with spatially programmable mechanical properties, allowing the same base material to express different effective stiffness, compliance, and energy absorption through geometry. TPMS families such as Gyroid, Diamond, IWP, and Primitive have attracted interest because their continuous surfaces can produce smooth load paths and tunable porous architectures [3-6, 15, 16]. In parallel, additive manufacturing of foot and ankle orthoses and 3D printed insole workflows have shown that patient-specific geometry and regional stiffness modulation are technically feasible [7-9, 13, 14]. These properties are attractive for insole design: the heel may require energy absorption, the midfoot may require supportive stiffness, and the forefoot may require compliance for comfort. Yet the existence of a programmable mechanical design space does not solve the mapping problem. A method is still needed to decide which structure should be assigned to each plantar region for each pressure phenotype.

The central gap addressed in this study is therefore not the measurement of plantar pressure alone or the generation of TPMS structures alone. The unresolved problem is the intermediate algorithm that converts pressure phenotypes into regional functional requirements and then matches those requirements to a mechanical structure database. Without this intermediate layer, design decisions remain dependent on experience, manual interpretation, or single-objective rules. For computationally designed insoles to become reproducible and explainable, the mapping between biological function and metamaterial mechanics should be explicit.

We propose MetaInsole Mapper, a phenotype-constrained multi-objective algorithm for programmable metamaterial insole design. The algorithm accepts a plantar pressure phenotype, constructs region-specific demand vectors, normalizes mechanical features from a TPMS database, and optimizes heel, midfoot, and forefoot assignments using functional matching scores and engineering penalties. The goal is to create a transparent computational design framework that can be inspected, reproduced, and extended. We tested whether MetaInsole Mapper could generate phenotype-specific regional TPMS assignments, outperform simple baseline assignment strategies, and remain stable under perturbations to the subjective demand weights.

2. MATERIALS AND METHODS

2.1. Study Design

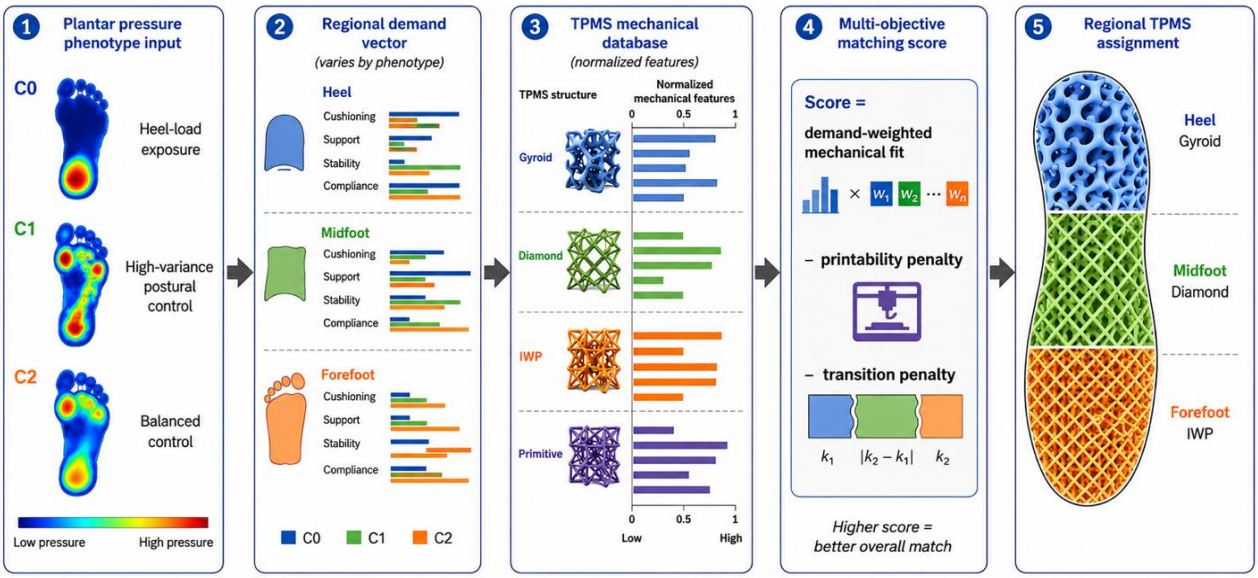

Figure 1. MetaInsole Mapper algorithm workflow

This was a computational design study. The input data consisted of a preprocessed plantar pressure phenotype summary and an existing TPMS mechanical database. The output was a phenotype-specific regional assignment of TPMS structures for three insole regions: heel, midfoot, and forefoot. The study did not include fabrication, bench testing of the final insole, or human wear validation. The purpose was to establish and evaluate the algorithmic mapping layer that links plantar pressure phenotype to programmable metamaterial structure selection.

The complete workflow is shown in Fig. 1. Plantar pressure phenotypes were encoded as regional demand vectors. TPMS structures were encoded as normalized mechanical feature vectors. A multi-objective score was then computed for each phenotype-region-structure combination. Final three-region assignments were selected by maximizing the total functional score while penalizing printability risk and abrupt stiffness transitions between adjacent regions.

2.2. Plantar Pressure Phenotype Input

Table 1. Plantar pressure phenotype inputs used by MetaInsole Mapper

Phenotype	n	Main signature	Design implication
C0	31	High heel PTI	Heel cushioning and load attenuation
C1	19	High total temporal variance	Stability and support enhancement
C2	50	Balanced standing control	General comfort and balanced support

The plantar pressure input was derived from a high-resolution quiet-standing dataset comprising 100 participants, three trials per participant, and 300 total trials. Each trial contained 3000 frames of 180 x 180 plantar pressure matrices. Previously extracted features included regional pressure, pressure-time integral, temporal variance, left-right load distribution, anterior-posterior load ratio, medial-lateral load ratio, arch load index, and center-of-pressure descriptors, consistent with common plantar-pressure assessment concepts [10, 11]. Unsupervised clustering identified three functional plantar pressure phenotypes.

The three phenotypes were used as the biological constraint layer for MetaInsole Mapper. Cluster C0 included 31 subjects and was interpreted as a heel cumulative-load exposure phenotype, characterized primarily by elevated heel pressure-time integral. Cluster C1 included 19 subjects and was interpreted as a high-variance postural-control phenotype, characterized primarily by elevated total temporal variance. Cluster C2 included 50 subjects and represented a relatively balanced quiet-standing control phenotype. These phenotypes were not treated as diagnostic categories; they were treated as computational design states that imply different regional mechanical priorities.

2.3. TPMS Mechanical Database

The TPMS input database contained 24 structures spanning Gyroid, Diamond, IWP, and Primitive architectures at different relative densities and unit sizes. Each structure had simulated force-displacement behavior summarized at multiple compression levels. The database fields used by the mapper included structure identifier, TPMS type, relative density, unit size, initial stiffness, apparent elastic modulus, force at 20% and 30% compression, energy absorption at 20% and 30% compression, convergence status, fallback count, and qualitative collapse behavior notes.

The database was converted into a manuscript-ready file, tpms_mechanical_database.csv, and a normalized feature table, tpms_normalized_feature_vectors.csv. Mechanical values were treated as relative computational descriptors within the current database rather than as universal material constants. This distinction is important because absolute values depend on the simulation setup, base material assumptions, sample geometry, and boundary conditions.

2.4. Regional Demand Vectors

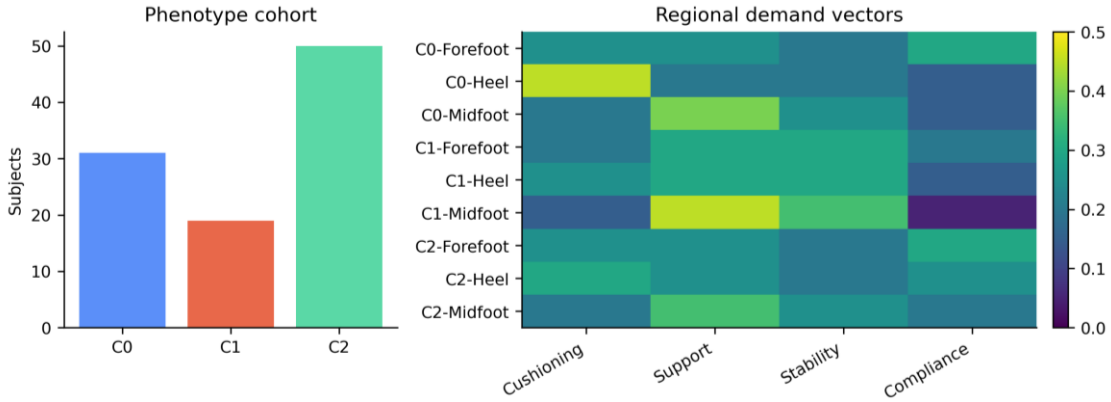

Figure 2. Pressure phenotype inputs and regional design demands

Each phenotype-region pair was encoded as a four-dimensional demand vector:

$$D\_\{p,r\} = [d\_c, d\_s, d\_t, d\_f], \quad \sum\_j d\_j = 1$$

Where p denotes phenotype and r denotes plantar region. Cushioning represents energy absorption demand, support represents stiffness demand, stability represents load-bearing and postural-control demand, and compliance represents comfort-oriented deformability. The components of each vector sum to 1.0. These vectors served as phenotype constraints and were selected to reflect the biomechanical interpretation of the three clusters.

For C0, the heel was assigned the highest cushioning demand because the dominant phenotype signature was heel cumulative-load exposure. For C1, the midfoot and forefoot were assigned greater support and stability demand because the dominant signature was high temporal variance. For C2, demand vectors were more balanced, reflecting the control-like loading pattern. The demand-vector table is provided in phenotype_region_demand_vectors.csv and visualized in Fig. 2.

2.5. TPMS Mechanical Feature Vectors

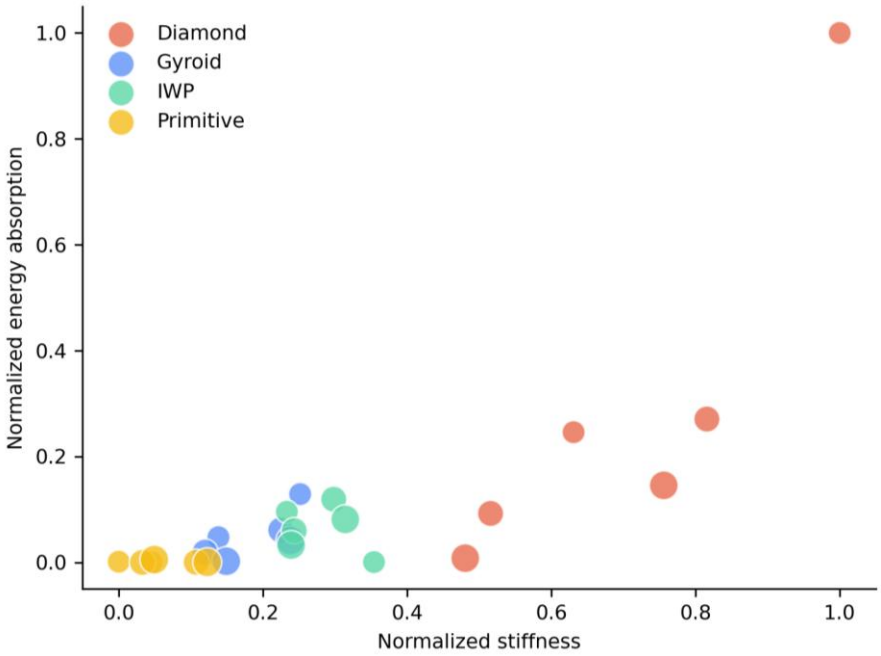

Figure 3. TPMS mechanical performance space

Each TPMS candidate structure was encoded as a four-dimensional mechanical feature vector:

$$M\_i = [m\_e, m\_k, m\_l, m\_f]$$

Energy Absorption was computed from normalized energy absorption at 20% compression. Stiffness was computed from normalized initial stiffness. LoadCapacity was computed from normalized force at 20% compression. Compliance was defined as the inverse normalized stiffness term:

$$m\_f(i) = 1 - m\_k(i)$$

Min-max normalization was applied within the 24-structure database so that all features ranged from 0 to 1. This allowed demand weights and mechanical features to be compared on a common scale. The resulting feature space is shown in Fig. 3. Because TPMS structures occupied distinct regions of the stiffness-energy absorption plane, the database was suitable for function-specific assignment.

2.6. Candidate Pools By Plantar Region

The algorithm used region-specific candidate pools to prevent mechanically implausible assignments. Heel candidates were selected from structures previously identified as high-cushioning candidates. Midfoot candidates were selected from high-support candidates. Forefoot candidates were selected from soft or compliant candidates. Each region had five candidate structures, yielding 125 possible heel-midfoot-forefoot combinations per phenotype. Region-specific pools were used as engineering constraints rather than as final rules; the final assignment was still determined by the multi-objective score.

2.7. Multi-objective Scoring

For a phenotype p, region r, and structure i, the base functional score was the dot product of the demand vector and the normalized mechanical feature vector:

$$S(p,r,i) = D\_\{p,r\} \cdot M\_i = d\_c\ m\_e(i) + d\_s\ m\_k(i) + d\_t\ m\_l(i) + d\_f\ m\_f(i)$$

Where d_c, d_s, d_t, and d_f are the demand weights for cushioning, support, stability, and compliance. The corresponding structure features are energy absorption (C_i), stiffness (S_i), load capacity (T_i), and compliance (F_i). This dot-product formulation makes the score interpretable: the selected structure is favored when its mechanical feature profile aligns with the regional functional demand.

2.8. Printability Penalty

A printability-risk penalty was included to discourage structures with higher engineering risk. The penalty combined fallback count, qualitative collapse indicators, force-drop behavior, densification behavior, and relative-density extremes. The risk score was clipped to the range 0 to 1 and converted to printability as:

$$Q\_i = 1 - R\_i$$

The printability penalty coefficient was set to 0.12 in the default mapper. This coefficient was deliberately modest: it could alter close choices, but it did not dominate the functional demand score.

2.9. Adjacent-region Transition Penalty

Because a practical insole should avoid abrupt mechanical discontinuities between adjacent regions, a transition penalty was computed from normalized stiffness differences between the heel, midfoot, and forefoot assignments:

$$P\_a = |m\_k(a\_H) - m\_k(a\_M)| + |m\_k(a\_M) - m\_k(a\_F)|$$

Where K is normalized stiffness. The transition penalty coefficient was set to 0.05. This value preserved phenotype-specific choices while discouraging excessive stiffness jumps. Higher transition coefficients were found to reduce phenotype specificity by pulling multiple phenotypes toward the same assignment.

2.10. Three-region Assignment Optimization

Final assignments were optimized at the three-region combination level rather than by independent greedy selection. For each phenotype, all candidate combinations were enumerated. The final objective was:

$$F(p,a) = \sum\_\{r \in R\} [S(p,r,a\_r) - \lambda_1\ R\_\{a\_r\}] - \lambda_2\ P\_a$$

Where lambda_1 = 0.12 and lambda_2 = 0.05. The selected assignment was the combination with the highest final score. This formulation allowed a structure with a slightly lower local regional score to be selected if it improved the overall mechanical continuity of the insole.

2.11. Baseline Methods

MetaInsole Mapper was compared with three baseline methods. Random assignment selected a candidate structure independently for each region and phenotype from the region-specific candidate pools. Results were averaged over 300 random iterations. Uniform TPMS assignment selected one structure for all regions and phenotypes, representing a homogeneous metamaterial design. The pressure-only rule selected a structure according to the dominant demand dimension in each region without optimizing a full demand vector or transition penalty.

Four comparison metrics were computed. Demand-matching error quantified the mismatch between demand-weighted functional expectation and assigned structure performance after printability and feasibility penalties. Functional score was the total demand-weighted objective score after penalties. Regional specificity measured whether heel, midfoot, and forefoot received distinct structures. Phenotype specificity measured whether assignments differed across phenotypes.

2.12. Sensitivity and Ablation Analyses

Sensitivity analysis tested whether assignments depended excessively on subjective demand weights. Demand-vector components were perturbed by +/-5%, +/-10%, and +/-20%, followed by renormalization so that each vector summed to 1.0. Sixty perturbation iterations were run at each level. Stability was defined as the fraction of region-level assignments that matched the unperturbed baseline assignment.

Ablation analysis tested the contribution of major algorithm components. The full mapper was compared with three ablated variants: removal of phenotype constraints, removal of transition penalty, and removal of printability penalty. Each ablation was evaluated using the same metrics as the baseline comparison.

3. RESULTS

3.1. Plantar Pressure Phenotypes Define Distinct Regional Design Demands

The phenotype input layer converted three plantar pressure clusters into explicit regional design demands (Fig. 2). C0 was associated with high heel pressure-time integral and was therefore assigned the strongest heel cushioning demand. C1 was associated with elevated temporal variance and was assigned greater support and stability demand, particularly in the midfoot. C2 represented a balanced quiet-standing control phenotype and was assigned more evenly distributed demands. This encoding step made the biological interpretation of each cluster visible to the algorithm rather than leaving it as an informal design judgment.

3.2. TPMS Structures Form A Programmable Mechanical Feature Space

The normalized TPMS feature space showed that the 24 structures spanned distinct regions of stiffness and energy absorption (Fig. 3). Diamond structures occupied the high-stiffness and high-load-capacity portion of the database, making them suitable candidates for midfoot support. Primitive structures occupied the high-compliance, low-stiffness region, making them suitable for comfort-oriented forefoot assignment. Gyroid and IWP structures provided intermediate feature combinations and contributed to heel cushioning and balanced assignments. This distribution supports the premise that TPMS structures can be treated as a programmable mechanical library for regional insole design.

3.3. MetaInsole Mapper Generates Phenotype-Specific Regional Assignments

Table 2. Final phenotype-specific regional TPMS assignments

Phenotype	Heel assignment	Midfoot assignment	Forefoot assignment	Total final score	Transition penalty
C0	D30_U1.5	D20_U1	P30_U1.5	1.2198	1.4515
C1	D30_U1.5	D20_U1	P40_U1	1.2751	1.3616
C2	IWP40_U1	D20_U1	P30_U1.5	1.2371	1.6530

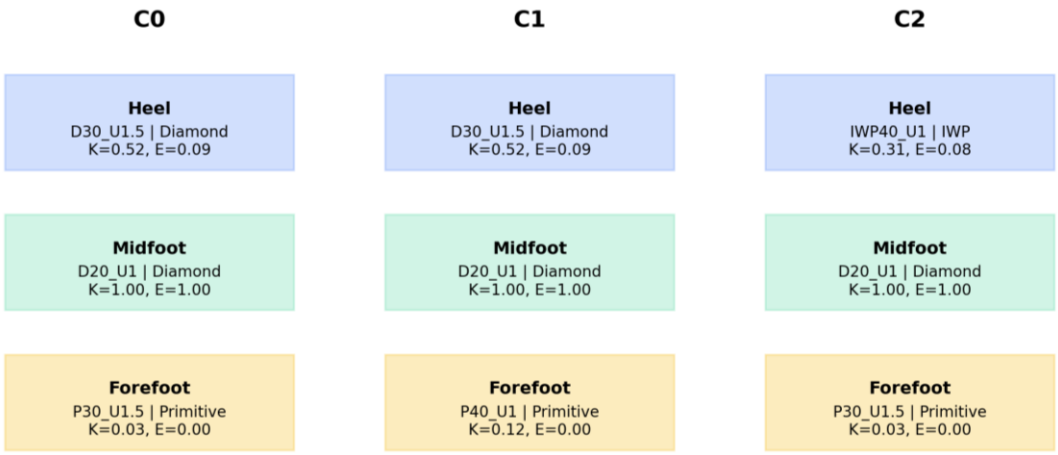

Figure 4. Phenotype-specific regional TPMS assignments

MetaInsole Mapper generated distinct regional TPMS assignments for the three phenotypes (Fig. 4). For C0, the selected heel, midfoot, and forefoot structures were D30_U1.5, D20_U1, and P30_U1.5, respectively. This assignment combined a moderate Diamond heel structure, a high-support Diamond midfoot structure, and a compliant Primitive forefoot structure. For C1, the selected structures were D30_U1.5, D20_U1, and P40_U1. The retained high-support midfoot assignment reflected the stability and support emphasis of the high-variance phenotype, while the forefoot shifted to a slightly stiffer Primitive structure than C0. For C2, the selected structures were IWP40_U1, D20_U1, and P30_U1.5, indicating a more balanced heel choice while retaining midfoot support and forefoot compliance.

The total final scores were 1.2198 for C0, 1.2751 for C1, and 1.2371 for C2. Transition penalties were 1.4515, 1.3616, and 1.6530, respectively. These values show that the final designs were not simply the best local choice in each region; they reflected the combination-level tradeoff between functional matching, printability risk, and stiffness continuity.

3.4. MetaInsole Mapper Outperforms Baseline Assignment Strategies

Table 3. Baseline comparison

Method	Demand-matching error	Functional score	Regional specificity	Phenotype specificity
Random assignment	0.7001	0.8435	0.9811	0.7926
Uniform TPMS	0.7040	0.8879	0.0000	0.0000
Pressure-only rule	0.5745	1.1948	1.0000	0.4444
MetaInsole Mapper	0.5605	1.2440	1.0000	0.4444

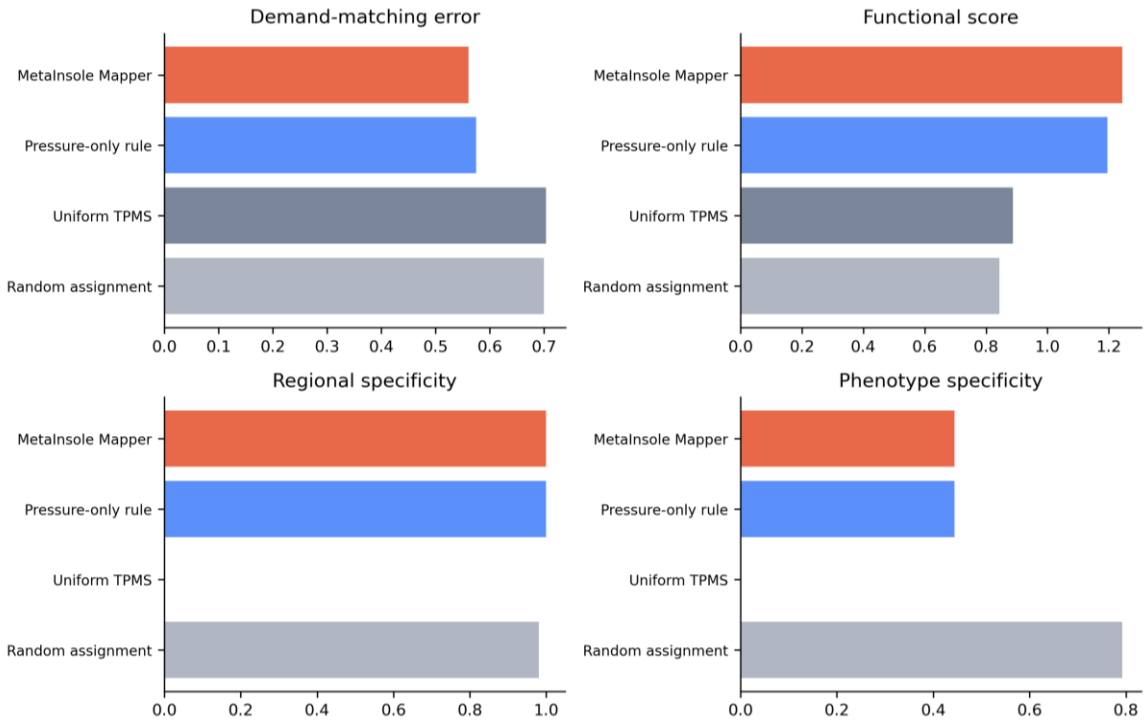

Figure 5. Baseline comparison across demand matching, functional score, regional specificity, and phenotype specificity

The proposed mapper outperformed all baseline methods on the two primary performance metrics (Fig. 5). Random assignment produced a demand-matching error of 0.7001 and a functional score of 0.8435. Uniform TPMS assignment produced a demand-matching error of 0.7040 and a functional score of 0.8879, with no regional or phenotype specificity. The pressure-only rule improved performance relative to random and uniform strategies, producing a demand-matching error of 0.5745 and a functional score of 1.1948. MetaInsole Mapper achieved the lowest demand-matching error (0.5605) and highest functional score (1.2440).

Both MetaInsole Mapper and the pressure-only rule achieved full regional specificity because they assigned different structures to heel, midfoot, and forefoot. However, MetaInsole Mapper improved functional score by optimizing the complete demand vector and including engineering penalties rather than selecting structures from only the dominant regional demand dimension. This result supports the value of multi-objective matching over single-rule assignment.

3.5. Sensitivity Analysis Supports Assignment Robustness

Table 4. Demand-weight perturbation sensitivity analysis

Perturbation level	C0 stability	C1 stability	C2 stability	Overall assignment stability
+/-5%	1.0000	1.0000	1.0000	1.0000
+/-10%	0.9833	1.0000	0.9778	0.9870
+/-20%	0.8778	0.9889	0.9333	0.9333

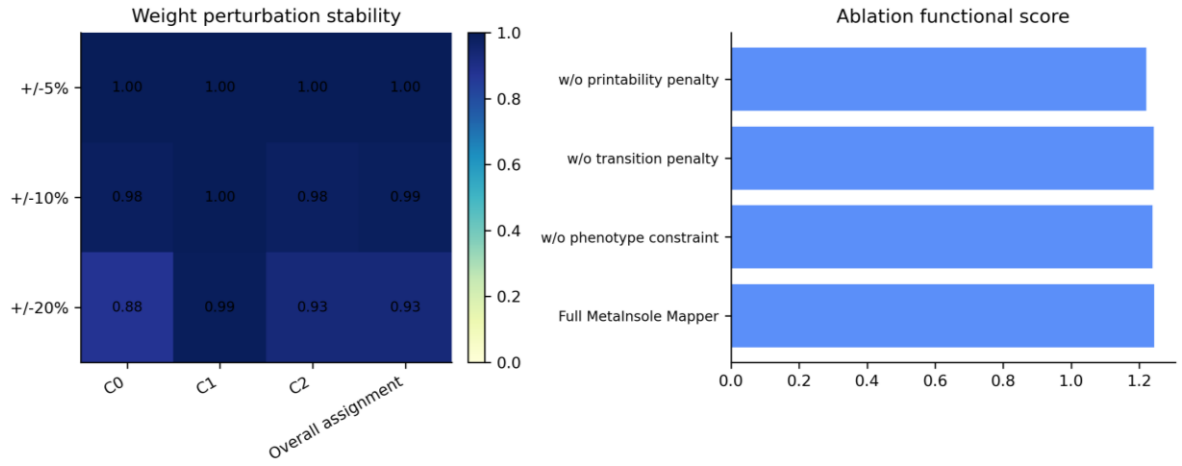

Figure 6. Sensitivity and ablation analyses

The assignment was stable under demand-weight perturbation (Fig. 6). At +/-5% perturbation, all phenotype assignments were unchanged, yielding an overall assignment stability of 1.0000. At +/-10% perturbation, overall stability remained high at 0.9870. At +/-20% perturbation, overall stability was 0.9333, with phenotype-level stability of 0.8778 for C0, 0.9889 for C1, and 0.9333 for C2. These results indicate that the algorithm was not driven by a fragile single weight value. The C1 assignment was particularly stable, consistent with the strong support and stability demand encoded for that phenotype.

3.6. Ablation Analysis Shows Contributions of Phenotype and Engineering Constraints

Ablation analysis showed that each major module contributed to the design behavior (Fig. 6). Removing phenotype constraints reduced phenotype specificity to 0.0000, confirming that phenotype-conditioned demand vectors were necessary to generate phenotype-specific designs. Removing the transition penalty slightly increased local demand matching but reduced the combination-level functional score, showing the expected tradeoff between regional optimality and global mechanical continuity. Removing the printability penalty decreased functional score and reduced phenotype specificity, indicating that the engineering-risk term influenced structure selection in close comparisons.

4. DISCUSSION

This study introduced MetaInsole Mapper, an interpretable algorithm for converting plantar pressure phenotypes into programmable metamaterial insole assignments. The main finding is that a compact phenotype-constrained, multi-objective formulation can connect two design spaces that are often treated separately: plantar pressure function and TPMS structural mechanics. The algorithm converted pressure-derived phenotypes into regional functional demand vectors, transformed TPMS simulation outputs into normalized mechanical features, and selected heel, midfoot, and forefoot structures through a combination-level objective.

The results support the central hypothesis that plantar pressure phenotypes can be used as computational constraints for regional insole design. C0, C1, and C2 produced related but non-identical assignments, reflecting their different functional signatures. The high-variance C1 phenotype retained the highest support emphasis, whereas the balanced C2 phenotype shifted toward a different heel structure. This phenotype-specific behavior is important because it moves the design process away from a single universal lattice or a purely pressure-magnitude rule. Instead, the algorithm exposes why a particular structure was selected for a particular region and phenotype.

The baseline comparison clarifies the contribution of the multi-objective formulation. Uniform assignment performed poorly because one structure cannot simultaneously satisfy heel cushioning, midfoot support, and forefoot compliance. Random assignment occasionally produced regional variation but lacked functional targeting. The pressure-only rule performed better because it used regional demand information, but it still ignored the full demand vector and transition-level optimization. MetaInsole Mapper improved on this rule by evaluating multiple mechanical dimensions simultaneously and by penalizing engineering risks. This is a practical advantage for design workflows: engineers can inspect the demand weights, feature scores, and penalties rather than accepting a black-box assignment.

The use of TPMS structures is also central to the framework. Prior studies of lattice and TPMS materials have shown that topology, relative density, unit-cell geometry, and grading strategy can strongly influence stiffness, energy absorption, and deformation behavior [3-6, 15, 16]. These properties make TPMS structures attractive for orthotic applications because they allow regional mechanical programming without changing the base material. MetaInsole Mapper does not require a specific TPMS family; it requires only a candidate database with comparable mechanical descriptors. As larger experimental or simulation databases become available, the same mapping framework could be extended to additional topologies, graded structures, or patient-specific geometry.

The algorithm was intentionally kept interpretable. Deep generative models and continuous topology optimization could eventually produce more complex designs, but they would require larger datasets, careful validation, and stronger assumptions about manufacturing and clinical performance. At the current stage, a transparent multi-objective mapper is a more appropriate bridge between phenotype discovery and physical insole design. It allows the research question to be tested directly: can functional plantar pressure phenotypes be converted into region-specific metamaterial assignments using a reproducible computational rule?

Several limitations should be emphasized. First, the study is computational. The final assignments have not yet been fabricated, mechanically tested as full insole regions, or evaluated in human participants. Therefore, the results should not be interpreted as evidence of clinical efficacy or comfort. Second, the demand vectors were manually specified from biomechanical interpretation of the phenotypes. Although sensitivity analysis showed robustness to perturbation, future work should estimate these weights from empirical outcomes, expert consensus, or optimization against target pressure reductions. Third, the TPMS database contained 24 structures, which is sufficient for proof-of-concept mapping but limited relative to the full design space of topology, density, cell size, grading, and material selection. Fourth, the printability penalty was a proxy based on simulation fallback and collapse indicators. Actual manufacturing feasibility should be evaluated through printing trials and mechanical tests.

Future work should proceed in three steps. The first step is fabrication validation: print the selected regional structures and measure stiffness, energy absorption, cyclic durability, and deformation under physiologically relevant loads. The second step is integrated insole testing: assemble regional designs into full insole prototypes and measure interface pressure under standing and walking, following the broader literature on pressure assessment and orthotic material evaluation [10, 12]. The third step is phenotype-guided human evaluation: test whether individuals assigned to C0, C1, or C2 receive differential pressure redistribution or comfort benefit from their mapped design. These studies would determine whether the computational mapping advantage observed here translates into mechanical and functional benefit.

5. SUMMARY

MetaInsole Mapper provides a reproducible algorithmic framework for translating plantar pressure phenotypes into regional programmable metamaterial insole designs. By encoding phenotype-region

demand vectors, normalizing TPMS mechanical features, and optimizing assignments with printability and transition penalties, the mapper generated interpretable phenotype-specific designs. Compared with random, uniform, and pressure-only baselines, it achieved lower demand-matching error and higher functional score while maintaining regional specificity and high sensitivity stability. The framework establishes a computational design bridge between plantar pressure phenotyping and TPMS metamaterial selection, setting the stage for fabrication and human validation.

DATA AND CODE AVAILABILITY

The executable analysis script is available in the project workspace as scripts/ run_metainsole_mapper.py. Generated data tables and figures are available under data/metainsole_mapper/. The current manuscript uses outputs generated from the existing plantar pressure phenotype summary and TPMS mechanical database in this workspace.

ETHICS STATEMENT

This manuscript draft is based on de-identified computational outputs available in the project workspace. Institutional review board approval, informed consent language, and any participant-protection statement from the original plantar pressure data collection should be inserted before journal submission if required by the target journal.

REFERENCES

[1] Bus, S. A., Waaijman, R., Arts, M., de Haart, M., Busch-Westbroek, T., van Baal, J., et al. (2013). Effect of custom-made footwear on foot ulcer recurrence in diabetes: a multicenter randomized controlled trial. Diabetes Care, 36(12), 4109–4116. https://doi.org/10.2337/dc13-0816

[2] Waaijman, R., de Haart, M., Arts, M. L. J., Wever, D., Verlouw, A. J. W. E., Nollet, F., & Bus, S. A. (2014). Risk factors for plantar foot ulcer recurrence in neuropathic diabetic patients. Diabetes Care, 37(6), 1697–1705. https://doi.org/10.2337/dc13-2476

[3] Melchels, F. P. W., Bertoldi, K., Gabbrielli, R., Velders, A. H., Feijen, J., & Grijpma, D. W. (2010). Mathematically defined tissue engineering scaffold architectures prepared by stereolithography. Biomaterials, 31(27), 6909–6916. https://doi.org/10.1016/j.biomaterials.2010.05.060

[4] Maskery, I., Aboulkhair, N. T., Aremu, A. O., Tuck, C. J., & Ashcroft, I. A. (2017). Compressive failure modes and energy absorption in additively manufactured double gyroid lattices. Additive Manufacturing, 16, 24–29. https://doi.org/10.1016/j.addma.2017.04.003

[5] Al-Ketan, O., Rowshan, R., & Abu Al-Rub, R. K. (2018). Topology-mechanical property relationship of 3D printed strut, skeletal, and sheet based periodic metallic cellular materials. Additive Manufacturing, 19, 167–183. https://doi.org/10.1016/j.addma.2017.12.006

[6] Gibson, L. J., & Ashby, M. F. (1997). Cellular Solids: Structure and Properties (2nd ed.). Cambridge University Press.

[7] Telfer, S., & Woodburn, J. (2010). The use of 3D surface scanning for the measurement and assessment of the human foot. Journal of Foot and Ankle Research, 3, 19. https://doi.org/10.1186/1757-1146-3-19

[8] Hudak, Y. F., Li, J. S., Cullum, S., Strzelecki, B. M., Richburg, C., Kaufman, G. E., et al. (2022). A novel workflow to fabricate a patient-specific 3D printed accommodative foot orthosis with personalized latticed metamaterial. Medical Engineering & Physics, 104, 103802. https://doi.org/10.1016/j.medengphy.2022.103802

[9] Nickerson, K. A., Li, E. Y., Telfer, S., Ledoux, W. R., & Muir, B. C. (2024). Exploring the mechanical properties of 3D-printed multilayer lattice structures for use in accommodative insoles. Journal of the Mechanical Behavior of Biomedical Materials, 150, 106309. https://doi.org/10.1016/j.jmbbm.2024.106309

[10] Orlin, M. N., & McPoil, T. G. (2000). Plantar pressure assessment. Physical Therapy, 80(4), 399–409. https://doi.org/10.1093/ptj/80.4.399

[11] Cavanagh, P. R., & Rodgers, M. M. (1987). The arch index: a useful measure from footprints. Journal of Biomechanics, 20(5), 547–551. https://doi.org/10.1016/0021-9290(87)90255-7

[12] Gerrard, J. M., Bonanno, D. R., Whittaker, G. A., & Landorf, K. B. (2020). Effect of different orthotic materials on plantar pressures: a systematic review. Journal of Foot and Ankle Research, 13, 35. https://doi.org/10.1186/s13047-020-00401-3

[13] Telfer, S., Pallari, J., Munguia, J., Dalgarno, K., McGeough, M., & Woodburn, J. (2012). Embracing additive manufacture: implications for foot and ankle orthosis design. BMC Musculoskeletal Disorders, 13, 84. https://doi.org/10.1186/1471-2474-13-84

[14] Daryabor, A., Kobayashi, T., Saeedi, H., & Lyons, S. M. (2023). Effect of 3D printed insoles for people with flatfeet: a systematic review. Assistive Technology, 35(1), 65–74. https://doi.org/10.1080/10400435.2022.2105438

[15] Yang, L., Ferrucci, M., Mertens, R., Dewulf, W., Yan, C., Shi, Y., et al. (2020). An investigation into the effect of gradients on the manufacturing fidelity of triply periodic minimal surface structures with graded density fabricated by selective laser melting. Journal of Materials Processing Technology, 275, 116367. https://doi.org/10.1016/j.jmatprotec.2019.116367

[16] Zhang, L., Feih, S., Daynes, S., Chang, S., Wang, M. Y., Wei, J., et al. (2021). Mechanical properties and energy absorption capability of graded-thickness triply periodic minimal surface structures fabricated by selective laser melting. International Journal of Mechanical Sciences, 204, 106586. https://doi.org/10.1016/j.ijmecsci.2021.106586